Title

Isoform-selective Genetic Inhibition of Constitutive Cytosolic Hsp70 Activity Promotes Client Tau Degradation Using an Altered Co-chaperone Complement*

Journal

Journal of Biological Chemistry, 290(21)

ISSN

0021-9258

Authors

Fontaine, Sarah N
Rauch, Jennifer N
Nordhues, Bryce A
et al.

Publication Date

2015-05-01

DOI

10.1074/jbc.m115.637595

Peer reviewed

THE JOURNAL OF BIOLOGICAL CHEMISTRY VOL. 290, NO. 21, pp. 13115–13127, May 22, 2015
Published in the U.S.A.

Isoform-selective Genetic Inhibition of Constitutive Cytosolic Hsp70 Activity Promotes Client Tau Degradation Using an Altered Co-chaperone Complement*

Received for publication, January 9, 2015, and in revised form, April 10, 2015 Published, JBC Papers in Press, April 11, 2015, DOI 10.1074/jbc.M115.637595

Sarah N. Fontaine[‡§], Jennifer N. Rauch[¶‖], Bryce A. Nordhues[‡§], Victoria A. Assimon[‖], Andrew R. Stothert[‡], Umesh K. Jinwal[**], Jonathan J. Sabbagh[‡§], Lyra Chang[‖], Stanley M. Stevens, Jr.[¶], Erik R. P. Zuiderweg[‡‡], Jason E. Gestwicki[‖], and Chad A. Dickey[‡§1]

*From the [‡]Department of Molecular Medicine, College of Medicine, USF Health Byrd Alzheimer's Institute, University of South Florida, Tampa, Florida 33613, [§]James A. Haley Veteran's Hospital, Tampa, Florida 33612, **Department of Pharmaceutical Science, College of Pharmacy, USF Health Byrd Alzheimer's Institute, University of South Florida, Tampa, Florida 33613, [¶]Deparment of Cell Biology, Microbiology and Molecular Biology, University of South Florida, Tampa, Florida 33620, [‖]Institute for Neurodegenerative Disease, University of California, San Francisco, California 94158, and [‡‡]Department of Biological Chemistry, University of Michigan, Ann Arbor, Michigan 48109*

Background: High levels of constitutive heat shock protein 70 (Hsc70) preserve Tau levels, possibly contributing to neuropathology.
Results: A dominant negative Hsc70 (DN-Hsc70) variant mimics small-molecule inhibition and facilitates Tau clearance by altering the associated interactome.
Conclusion: DN-Hsc70 recruits a pro-degradation chaperome complement to the Tau-Hsc70 complex.
Significance: Selective Hsc70 inhibition could have a therapeutic benefit in tauopathies including Alzheimer disease.

The constitutively expressed heat shock protein 70 kDa (Hsc70) is a major chaperone protein responsible for maintaining proteostasis, yet how its structure translates into functional decisions regarding client fate is still unclear. We previously showed that Hsc70 preserved aberrant Tau, but it remained unknown if selective inhibition of the activity of this Hsp70 isoform could facilitate Tau clearance. Using single point mutations in the nucleotide binding domain, we assessed the effect of several mutations on the functions of human Hsc70. Biochemical characterization revealed that one mutation abolished both Hsc70 ATPase and refolding activities. This variant resembled the ADP-bound conformer at all times yet remained able to interact with cofactors, nucleotides, and substrates appropriately, resembling a dominant negative Hsc70 (DN-Hsc70). We then assessed the effects of this DN-Hsc70 on its client Tau. DN-Hsc70 potently facilitated Tau clearance via the proteasome in cells and brain tissue, in contrast to wild type Hsc70 that stabilized Tau. Thus, DN-Hsc70 mimics the action of small molecule pan Hsp70 inhibitors with regard to Tau metabolism. This shift in Hsc70 function by a single point mutation was the result of a change in the chaperome associated with Hsc70 such that DN-Hsc70 associated more with Hsp90 and DnaJ proteins, whereas wild type Hsc70 was more associated with other Hsp70 isoforms. Thus, isoform-selective targeting of Hsc70 could be a viable therapeutic strategy for tauopathies and possibly lead to new insights in chaperone complex biology.

Cellular protein metabolism relies on a network of molecular chaperones that ensure proper folding and sorting of a protein for its intended function. The major chaperones in the cell, the Hsp90[2] and Hsp70 families, along with their assorted co-chaperones facilitate folding of nascent peptide chains, refold incorrectly folded proteins, or if refolding fails, send the protein for degradation. Hsp70s are extremely well conserved, multidomain proteins consisting of a nucleotide binding domain (NBD) that regulates the binding of either ATP or ADP, a substrate-binding domain (SBD), and a C-terminal domain, containing a tetratricopeptide repeat domain. Exchange of ATP for ADP allosterically controls the refolding function of Hsp70s and their substrate affinity; binding of ATP stabilizes the NBD, resulting in a closed nucleotide binding cleft while simultaneously destabilizing the SBD, resulting in decreased substrate affinity due to a solvent-exposed hydrophobic cleft (1). ATP hydrolysis is stimulated by Hsp40/DnaJ proteins, a class of co-chaperones that is also crucial for presentation of structurally diverse clients to Hsp70s (2, 3). The exchange of ADP for ATP results in a relaxation of the SBD conformation, allowing substrates to disengage and new substrates to bind; for reviews, see Refs. 4 and 5.

* This work was supported, in whole or in part, by National Institutes of Health Grants NS073899 (to C. A. D.), 2R01NS059690 (to E. R. P. Z. and J. E. G.), and AG042813 (to J. E. G.) and Veterans Health Administration (VHA) Grant BX001637 (to C. A. D.).

[1] To whom correspondence should be addressed: Dept. of Molecular Medicine and James A. Haley Veteran's Hospital, 4001 E. Fletcher Ave MDC 36, Tampa, FL, 33613. Tel.: 813-396-0639; E-mail: cdickey@health.usf.edu.

[2] The abbreviations used are: Hsp, heat shock protein; Hsc, heat shock cognate protein; NBD, nucleotide binding domain; SBD, substrate binding domain; DN-Hsc70, dominant-negative heat shock cognate protein 70; TROSY, transverse relaxation optimized spectroscopy; HSQC, spectra heteronuclear single quantum coherence; AAV, adeno-associated virus; ANOVA, analysis of variance; FP, fluorescence polarization.

In addition to these refolding and degradation roles, members of the Hsp70 family of chaperones have other varied functions around the cell both constitutively as well as under conditions of cellular stress. There are ~10 isoforms of human Hsp70 proteins, including stress-inducible (Hsp72) and organelle-specific isoforms (Grp78, mortalin) (6, 7). The constitutively expressed isoform, Hsp73/Hsc70, accounts for 2% of proteins in cells (8) and has long been implicated in clathrin-mediated endocytosis (9–11). Hsc70 is involved in a large variety of other cellular processes including exocytosis (12), trafficking of nuclear hormone receptors (13), transport of proteins from the Golgi to the endoplasmic reticulum (14), antigen presentation (15), and cytoskeletal function (16, 17). A possible link between Hsc70 and microtubules is that the intrinsically disordered protein (IDP) Tau is a reported client of Hsc70 (18–20). Tau is a microtubule-associated protein that functions to stabilize the microtubule network in neurons, providing support to the cell during axonal transport and controlling essential steps in microtubule dynamics (21–23). However, Tau is best known for its aberrant hyperphosphorylation and accumulation in a number of neurodegenerative disorders termed tauopathies (24, 25) where it leads to the formation of Tau aggregates that are linked to cognitive deficits (26, 27).

Building on a possible role for Hsc70 in microtubule dynamics, we previously showed that Hsc70 coordinates with the microtubule-associated protein Tau to regulate microtubules (18–20). However, this relationship between Tau and Hsc70 can have untoward consequences in the aging brain as Hsc70 appears to contribute to the pathogenic accretion of Tau (28). We previously showed that overexpression of Hsc70 slowed Tau metabolism, an effect that could be overcome by small molecule pan Hsp70 inhibitors (28–30). But most Hsp70 small molecule inhibitors are not isoform-selective, and none is available that specifically target Hsc70, making it challenging to define the specific role of Hsc70 activity on the turnover of clients like Tau (31–36). Because Hsp70 isoforms appear to have opposing effects on Tau proteostasis, it is difficult to determine the impact of individual activities of Hsp70 isoforms on Tau biology (28). To answer the question about the role of Hsc70 activity on Tau turnover, we generated a mutant form of human Hsc70, E175S. Compared with wild type Hsc70, this variant lacked both refolding and ATPase activities, remained permanently in an ADP-bound conformation, and had a very different interactome that facilitated Tau reductions via the proteasome. These findings provide strong rationale to support the development of isoform-selective Hsp70 inhibitors for understanding Tau biology and possibly developing therapeutics around this target or its interaction partners.

Experimental Procedures

Reagents—Unless stated otherwise, all chemical reagents were purchased from Sigma.

Plasmids and Antibodies—For mammalian expression experiments, full-length human Hsc70 genes were cloned into pCMV6 (Origene, Rockville, MD) with an N-terminal FLAG tag to distinguish between endogenous and overexpressed isoforms. Mutations were introduced via site-directed mutagenesis (Stratagene, La Jolla, CA), and all sequences were verified before use. WT 4R0N Tau was cloned into pCDNA3.1+ as previously described (28). For recombinant protein preparations, WT-Hsc70, all Hsc70 mutants, and DnaJs were cloned into the pET28a vector (Midwest Center for Structural Genomics, Bethesda, MD).

The following antibodies were purchased commercially: Hsc70 (Stressgen, Enzo Life Sciences, Farmingdale, NY), TauH150 (Santa Cruz Biotechnology, Santa Cruz, CA), β-actin, tubulin, and M2-FLAG (Sigma), beclin-1 (Abcam, Cambridge, MA), and glyceraldehyde 3-phosphate dehydrogenase (GAPDH) (Cell Signaling Technologies, Danvers, MA).

Expression and Purification of Recombinant Proteins—Wild type 4R0N Tau, full-length Hsc70 (WT and E175S), and Hsc70 NBD fragments, DnaJ proteins, and BAG1 proteins were purified as described previously (28, 37). For expression of isotopically ^{15}N-labeled full-length wild type and E175S Hsc70 protein, expression plasmids were transformed into *Escherichia coli* OneShot BL21 Star (DE3) cells (Life Technologies, Carlsbad, CA), and starter cultures were grown overnight in Luria-Bertani medium with the appropriate antibiotic. Overnight cultures were centrifuged, and cells were resuspended in M9 minimal media supplemented with 1 g/liter [^{15}N]ammonium chloride, 100 μM $CaCl_2$, 100 μM $MgSO_4$, 0.4% (w/v) glucose, and trace metals and vitamins, then grown at 37 °C to an optical density of ~0.7 and induced with 1 mM isopropyl β-D-1-thiogalactopyranoside, and proteins were expressed at 37 °C for 3 h. The cells were then harvested by centrifugation at 4000 × *g* for 15 min at 4 °C and resuspended in lysis buffer (500 mM NaCl, 20 mM Tris-HCl, 5 mM imidazole, 1× protease inhibitor mixture III (EMD Millipore, Billerica, MA) and 1 mM phenylmethylsulfonyl fluoride, pH 8.0). Purification of protein from this resuspension was executed as described previously (28).

ATPase Activity for Hsc70—Intrinsic ATPase rate was measured via malachite green assay with human WT or mutant Hsc70 (0.6 μM) in the absence of co-chaperones or substrate as previously described (38, 39). Briefly, proteins were incubated with nucleotide exchange factors and J proteins as indicated, and reactions were performed in the presence of ATP for 1 h, developed with malachite green reagent, and quenched with sodium citrate, and the resulting absorbance at 620 nm was measured.

Luciferase-monitored Refolding Assay—The DnaJ-stimulated refolding activity was characterized as previously described (40). Briefly, guanidine HCl-denatured luciferase was diluted into a HEPES-buffered ATP regenerating system containing WT or E175S Hsc70. Various DnaJ proteins were added to stimulate the reaction, which was allowed to proceed for 1 h at 37 °C before measuring luminescence using the SteadyGlo reagent (Promega).

Fluorescence Polarization Assays—Fluorescence polarization experiments using the HLA-FAM (Anaspec) and ATP-FAM (Jena Bioscience) reporters were performed as described previously (37). Briefly, recombinant WT and E175S Hsc70 was incubated with reporter and florescence polarization was measured (excitation 485 nm, emission 535 nm) using a SpectraMax M5 plate reader.

Fluorescence Binding by Flow Cytometry—Experiments were performed as described (37). Briefly, biotinylated recombinant

WT and E175S Hsc70 were bound to streptavidin-coated polystyrene beads (Spherotech) in the presence of 1 mM nucleotide. Beads were washed and labeled BAG1 was applied. BAG1 binding was measured by quantification of bead-associated fluorescence by and Accuri C6 flow cytometer.

NMR Spectroscopy—The conformations of ^{15}N-labeled WT-Hsc70 and Hsc70-E175S were characterized in the ADP-Tau peptide VQIVYK-bound state and the ATP state. Typical concentration of the samples was 50 μM in protein. Hsc70-hydrolyzed ATP was recycled by a regeneration system consisting of 100 mM phosphocreatine and 20 units of phosphocreatine-ADP kinase. ^{1}H,^{15}N TROSY-HSQC spectra (transverse relaxation optimized spectroscopy-heteronuclear single quantum coherence) were collected at 700 or 900 MHz using a Bruker Avance III system equipped with a triple resonance cryo-probe (Michigan Research Corridor Facility at Michigan State University, East Lansing, MI). The TROSY spectra were collected in 10 h each, processed with NMRPipe, and plotted in Sparky (T. D. Goddard and D. G. Kneller, University of California, San Francisco, CA).

One-dimensional versions of the standard ^{15}N R_1 (10 h) HSQC experiments were carried out. The data set was processed in NMRPipe and exported in (ASCII) format using the Pipe2txt.tcl routine. The data were imported into Microsoft Excel and plotted. For each spectrum, the ranges 9.6–8.6 ppm (structured core residues) and 8.6–7.8 ppm (structured core and mobile tail residues) were integrated and fitted to a single exponential using in-house-written nonlinear least square fit code with jackknife error estimation (41). ^{15}N R_2 relaxation rates obtained from one-dimensional versions of a ^{15}N chemical shift anisotropy/^{1}H,^{15}N dipolar transverse cross-correlated relaxation, η_{xy}, were obtained using symmetric reconversion. Four spectra, $N_{xy} \rightarrow N_{xy}$, $N_{xy} \rightarrow 2N_{xy}H_z$, $2N_{xy}H_z \rightarrow N_{xy}$, and $2N_{xy}H_z \rightarrow 2N_{xy}H_z$, measuring the auto- and cross-correlated relaxation rates over a period T of 10.2 ms were collected in 5 h total and processed as described above. The rates η_{xy} were obtained from the equation,

$$\eta_{xy} = \frac{1}{2T}\ln((1 - R)/(1 + R)) \qquad \text{(Eq. 1)}$$

where R is given by,

$$R = \sqrt{\frac{I_{Nxy \rightarrow 2\,NxyHz} \times I_{2\,NxyHz \rightarrow Nxy}}{I_{Nxy \rightarrow Nxy} \times I_{2\,NxyHz \rightarrow 2\,NxyHz}}}$$

Cell Culture, Lysis, Co-immunoprecipitation, and Immunoblotting and Viability—HEK293T cells were maintained, transfected, harvested, and immunoblotted as described previously (28). Viability was measured by 3-(4,5-dimethylthiazol-2-yl)-5-(3-carboxymethoxyphenyl)-2-(4-sulfophenyl)-2H-tetrazolium (MTS) assay according to manufacturer's protocol (Promega, Madison, WI).

Organotypic Slice Culture, Transduction, and Immunofluorescence—All procedures involving experimentation on animal subjects were done in accordance with the guidelines set forth by the Institutional Animal Care and Use Committee of the University of South Florida. For slice cultures, post-natal day 5–9 FVB-Tg(tetO-MAPT*P301L) mice (The Jackson Laboratory, Bar Harbor, ME) were rapidly decapitated, and brains were sectioned at 400-μm thickness on a vibratome (Leica Microsystems, Buffalo Grove, IL) in 0.6% glucose-PBS, pH 7.4. This model produces excess mutant P301L human Tau that pathologically condenses to the perikarya as in human disease (27). Slices were immediately plated onto Millicell inserts (EMD Millipore) in 6-well plates (Corning) containing complete culture medium (DMEM/F-12, 2 mM Glutamax, penicillin/streptomycin, and 25% (v/v) heat-inactivated horse serum (Life Technologies)). Media was changed every 2–3 days. For adeno-associated virus (AAV), DIV2, slices were incubated with 10 μl of WT-Hsc70-FLAG, AAV9 E175S-Hsc70-FLAG, or AAV9-GFP at 10^{10} titer for 14 days. After transduction, slices were fixed, permeabilized, and blocked as described previously (42). Slices were incubated in the appropriate primary antibodies overnight followed by anti-goat Alexa-Fluor-conjugated secondary antibodies (Life Technologies). Nuclei were visualized with 4′,6-diamidino-2-phenylindole (DAPI) staining, then cover-slipped using ProLong antifade reagent (Life Technologies). Intensity analyses were performed with ImageJ.

siRNA-mediated Knockdown—siRNAs for human *BECN1* and controls were purchased from Qiagen (Buffalo Grove, IL). Knockdowns were performed for 72 h on HEK293T with 40 nM siRNA using silentFECT (Bio-Rad).

Statistical Analyses—Statistical analyses were performed by one-way ANOVA tests with Tukey's post-hoc analysis for multiple comparisons or Student's *t* tests, as indicated in the figure legends, using GraphPad Prism 5.0 software.

Results

A Human Hsc70 Variant Lacks ATPase and Refolding Activities—We mutated specific residues in the NBD domain of human Hsc70 that we supposed would alter the ATPase activity of Hsc70 based on literature and structure (43–45) (Fig. 1*A*). These variants were screened for *in vitro* ATP hydrolysis and luciferase refolding in the presence of the co-chaperone Hsp40/DnaJA2, which greatly enhances detection of these activities. Point mutations S208A, D152K, C267S, and F68L all demonstrated increased ATPase activity compared with WT Hsc70 (Fig. 1*B*). Only E175S Hsc70 lacked any appreciable ATPase activity compared with WT Hsc70 (Fig. 1*B*). We then assessed how these same point mutants impacted luciferase refolding activity. Interestingly, F68L Hsc70 increased luciferase refolding compared with WT, but E175S, D152K, and S208A Hsc70 variants had no refolding activity (Fig. 1*C*). The S208A and C267S mutations were able to refold luciferase similarly to WT. We then co-overexpressed each Hsc70 mutant with WT 4R0N Tau (Tau without any N-terminal inserts but four microtubule binding repeats) and assessed cellular Tau levels in HEK293T cells by Western blot (Fig. 1*D*) to understand which Hsc70 activity, ATPase or refolding, was most critical for Tau metabolism. Compared with mock-transfected samples, overexpression of WT Hsc70 preserved Tau levels in the cell as previously shown (28). Overexpression of E175S Hsc70 significantly decreased cellular Tau levels (Fig. 1, *D* and *E*; *, $p \leq 0.05$) as did D125K (Fig. 1, *D* and *E*). The S208A and C267S mutants had no

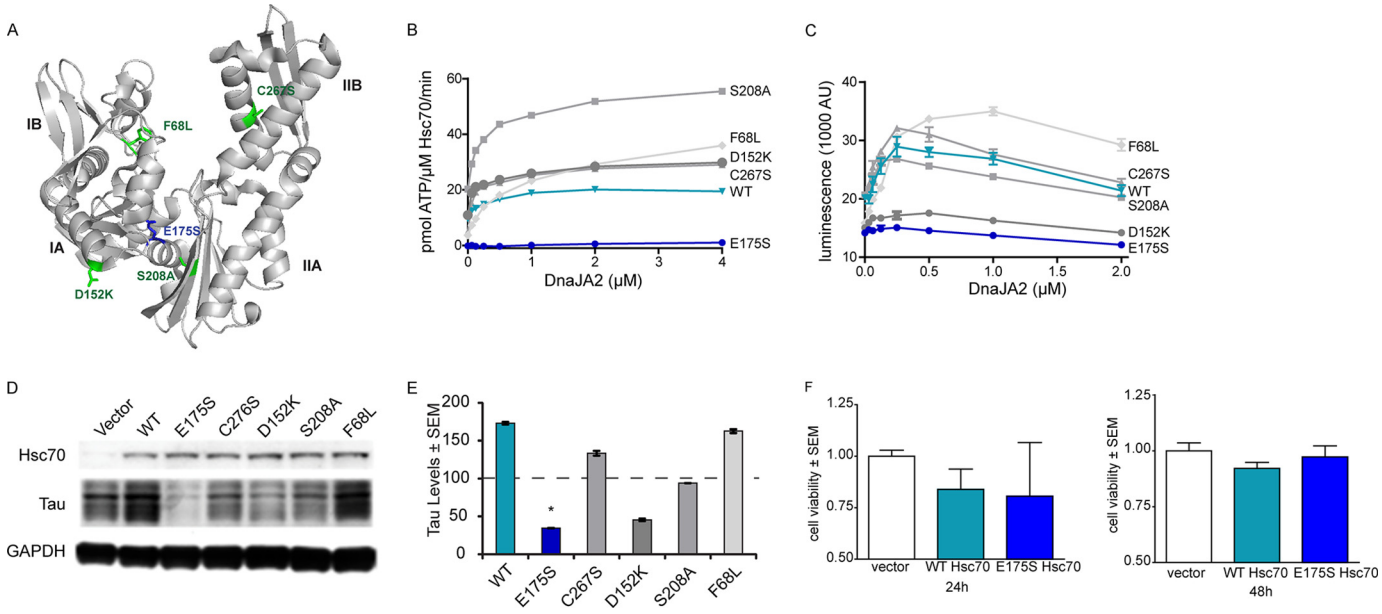

FIGURE 1. **Point mutations in Hsc70 mimicking small molecule inhibition variously affect Tau levels.** *A*, locations of point mutations the ribbon structure (PDB code 3FZF) of the ATP-bound Hsc70 NBD. E175S is *blue*; all other mutations are shown in *green*. *B*, *in vitro* ATPase activity of human Hsc70 NBD (amino acids 1–386) in the presence of DnaJA2. WT is shown in *cyan*, F68L, D152K, S208A, C267S are all in *gray*), and E175S is indicated in *blue*. *C*, screen of *in vitro* DnaJA2-stimulated luciferase refolding activity of human Hsc70 NBD (amino acids 1–386) of WT Hsc70 (*cyan*) compared with F68L, D152K, S208A, C267S (*all gray*) and E175S(*blue*) Hsc70. *AU*, absorbance units. *D*, representative Western blot HEK293T cells overexpressing Tau and each full-length Hsc70 variant compared with a mock control. Quantification of Tau levels are shown in *E* (mean ± S.D., $n = 3$), *, $p \leq 0.05$ by one-way ANOVA. *F*, overexpression of DN Hsc70 does not significantly alter the number of viable cells at 24 or 48 h. Data are the mean ± S.E., $n = 3$ independent repeats.

significant impact on Tau stability. We were intrigued by the E175S mutant, which lacked both luciferase and ATPase activities yet significantly impacted Tau levels. We next tested cell viability, which was not significantly affected by overexpression of E175S Hsc70 in Tau-expressing cells, ruling out the possibility that Tau levels decreased due to cell death (Fig. 1*F*). These findings demonstrate that Tau clearance is facilitated most robustly when Hsc70 lacks both primary refolding and ATPase activities. This was similar to what we had previously observed with small molecule pan Hsp70 inhibitors (30).

Further analysis revealed that E175S Hsc70 was not able to stimulate ATP hydrolysis irrespective of which DnaJ was used to stimulate the reaction (Fig. 2*A*). Then, using fluorescence polarization (FP), we found WT and E175S Hsc70 bound to the ATP-FAM reporter with similar K_d ranges (410 nM ± 20 nM for WT Hsc70 and 430 nM ± 40 nM for E175S Hsc70, Fig. 2*B*) eliminating any concerns that E175S Hsc70 was unable to hydrolyze ATP due to a deficiency in nucleotide binding. E175S Hsc70 had slightly reduced affinity for ADP compared with WT Hsc70 in nucleotide competition experiments but was otherwise normal (Fig. 2*B*). E175S Hsc70 and WT Hsc70 both bound to BAG1, the nucleotide exchange factor similarly, suggesting that the E175S mutation does not interrupt nucleotide exchange factor interactions (Fig. 2, *C* and *D*). Similar to what was observed with ATP binding, E175S Hsc70 could not refold luciferase regardless of which human DnaJ was present (Fig. 2*E*). Together, these data indicate that E175S Hsc70 is unable to cycle ATP or refold luciferase despite appropriately interacting with its co-factors, which suggests this variant may have dominant negative (DN) characteristics.

To further determine if E175S Hsc70 was in fact acting as a DN variant, which would almost exactly mimic isoform-selective inhibition (28), we sought to confirm that this variant could still bind substrate using FP assays with the tracer HLA-FAM (46). In these experiments we used Hsp72 as a comparison for E175S because apo-Hsp72 has superior FP signal to apo-WT Hsc70 for reasons that are not clear (Fig. 2*F*). Hsp72 bound the HLA-FAM tracer with a K_d of 23 μM in the ATP-bound state, whereas ADP addition improved the K_d to 2.0 μM ± 0.6 μM (Fig. 2*F*). In comparison, E175S Hsc70 had a high affinity for substrate regardless of nucleotide (with ATP, $K_d = 2.0$ μM ± 0.8 μM; with ADP, $K_d = 3.1$ μM ± 0.8 μM; Fig. 2*F*). These data indicated that E175S Hsc70 can bind substrate, but it is locked in an ADP-like conformation with high affinity for substrates. These data provide further evidence that E175S Hsc70 is a DN form of this protein, with properties that are identical to chemically inhibited Hsc70.

Structural Characterization of E175S Hsc70—Previous work suggests that inhibiting Hsc70 with a ligand altered the allosteric communication between the SBD and NBD of this protein (33, 47, 48). With this in mind, we performed 900-MHz TROSY NMR experiments comparing the ATP- and ADP-bound NBD (amino acids 1–386) of WT Hsc70 (*red*, *blue*) and ATP- and ADP-bound E175S Hsc70 (*orange*, *cyan*) (Fig. 3*A*) to assess the structural ramifications of the E175S mutation. Although both NBDs were globally well folded, a number of resonances were missing or shifted in the E175S mutant, indicating that it had undergone some structural rearrangement compared with WT Hsc70 (Fig. 3*B*). This effect was likely due to millisecond conformational exchange dynamics due to increased flexibility. Furthermore, these data confirm that E175S Hsc70 does undergo conformational change upon nucleotide binding, proving the mutant is still capable of binding nucleotide (Fig. 3*C*), but there are no significant structural differences between

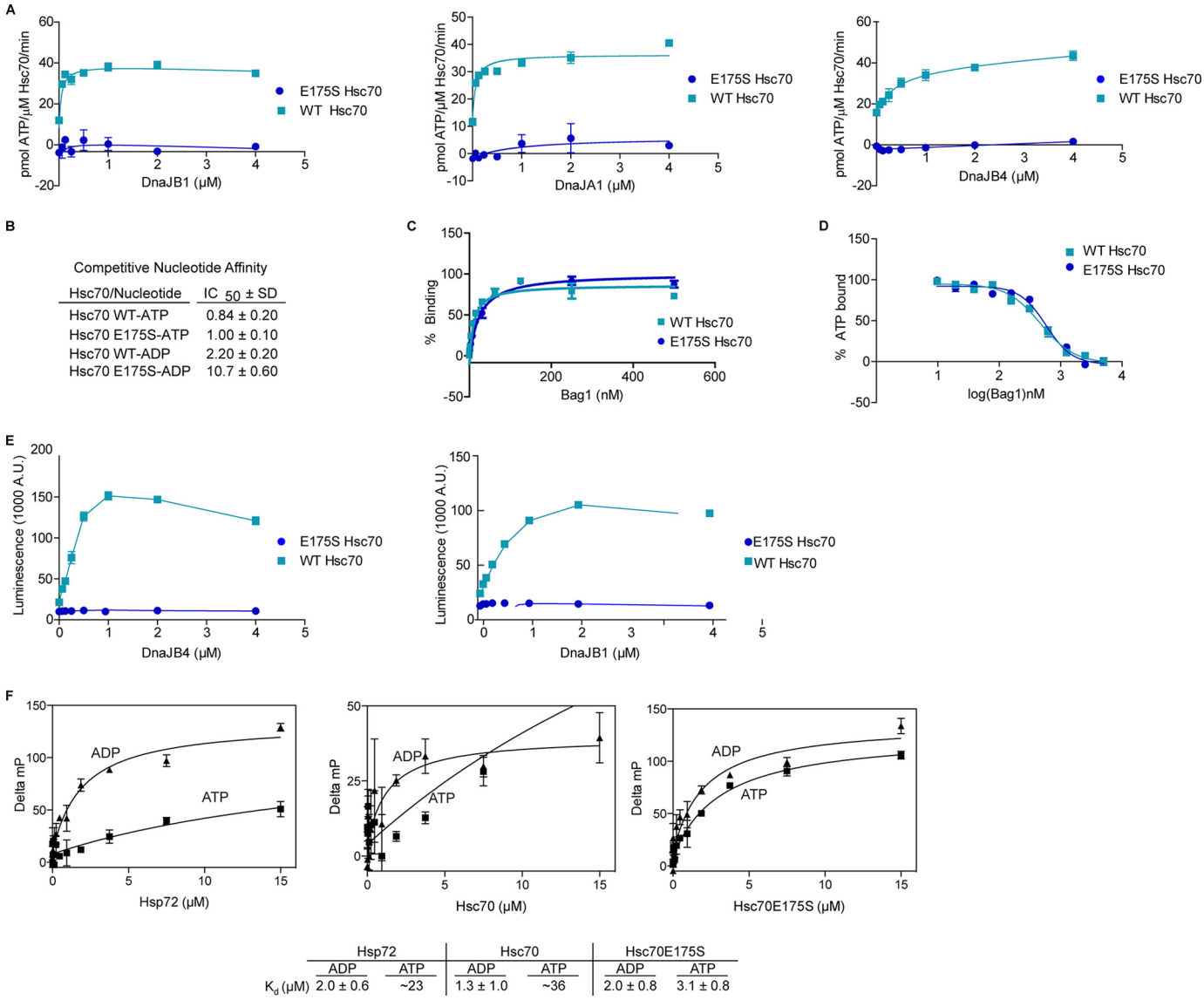

FIGURE 2. **E175S Hsc70 is a dominant negative Hsc70.** *A*, E175S Hsc70 (*blue*) lacks appreciable ATPase activity compared with WT Hsc70 (*cyan*) in reactions stimulated with DnaJA1, DnaJB1, or DnaJB4. Data are the means of three independent measurements. *B*, fluorescence polarization competition assays indicate both ATP and ADP outcompete ATP-FAM binding in E175S Hsc70, indicating the protein binds nucleotide. Data are the means of triplicate independent reactions. *C*, E175S Hsc70 (*blue*) does not differ in ability to bind BAG1 compared with WT Hsc70 (*cyan*) as measured by a flow cytometry protein interaction assay. *D*, E175S Hsc70 (*blue*) does not differ from WT Hsc70 (*cyan*) in BAG1-stimulated fluorescence polarization tracer (ATP-FAM) release competition experiments. Data are the means of three independent measurements. *E*, E175S (*blue*) cannot refold luciferase irrespective of DnaJ used to stimulate the reaction when compared with Hsc70 WT (*cyan*). *F*, Hsp72 WT or Hsc70 E175S with ATP and ADP or without nucleotide. The addition of ATP reduces substrate HLA-FAM tracer binding in Hsp72 but not Hsc70 E175S. Data represent the means.

the ATP and ADP state of E175S Hsc70 1–386 (Fig. 3*D*), in contrast to the conformational changes associated with the ATP *versus* ADP state of WT Hsc70 1–386 (Fig. 3, *E* and *F*). When the chemical shifts were mapped on the crystal structure of Hsc70 NBD (Fig. 3*G*), they clustered to subdomains IA and IIA adjacent to the mutation. In addition, some chemical shifts were also seen in subdomains IB and IIB, suggesting that the interfaces between subdomains may have been affected. However, despite these structural changes, E175S Hsc70 still functionally resembled a WT Hsc70 NBD, able to bind nucleotides and nucleotide exchange factors.

Based on these results, we sought to determine if the structural ramifications of the E175S Hsc70 variant were sufficient to prevent the allosteric communication between the NBD and SBD, perhaps explaining its functional profile. To test this idea, we turned to one-dimensional ^{1}H-detected HSQC experiments. Specifically, we measured ^{15}N spin relaxation rates for the amide-proton signals of Hsc70 (Fig. 4) in different nucleotide-bound states (49, 50) in the presence of a Tau peptide. ^{15}N relaxation rates provide insight into overall protein tumbling, which is influenced by shape and effective molecular weight. From this experiment, three regions were identified; the region of $^{1}H > 8.6$ ppm corresponds to structured protein, the region $8.6 > {}^{1}H > 7.6$ ppm is dominated by signals of the unstructured areas, and the region $^{1}H < 7.6$ ppm contains residual signals from structured side chains. As expected, the R_1 relaxation of the structured area was much slower than that of the unstructured area, corresponding to a larger rotational correlation time

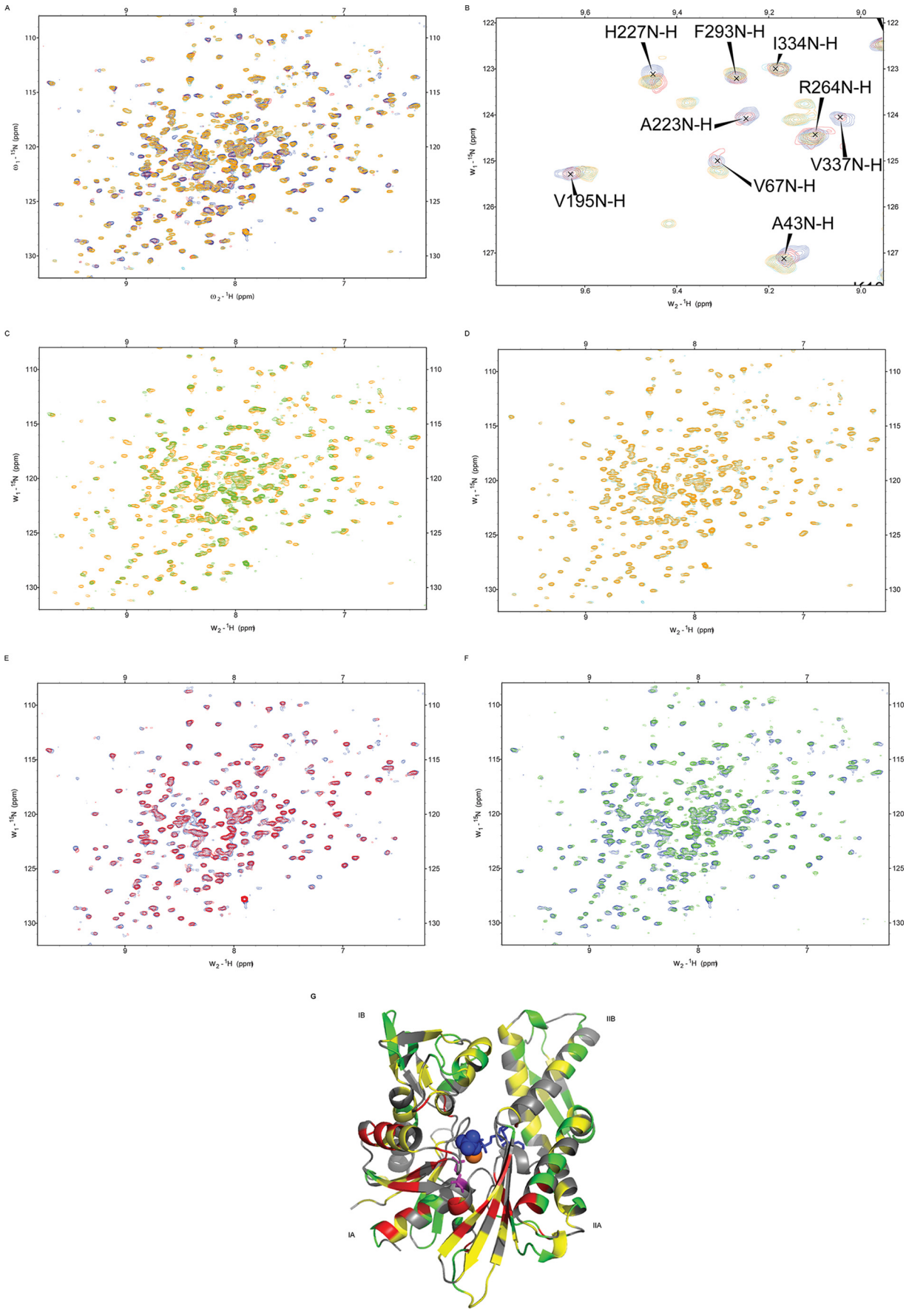
A
B
H227N-H
F293N-H
I334N-H
R264N-H
A223N-H
V337N-H
V67N-H
V195N-H
A43N-H
C
D
E
F
G
IB
IIB
IA
IIA

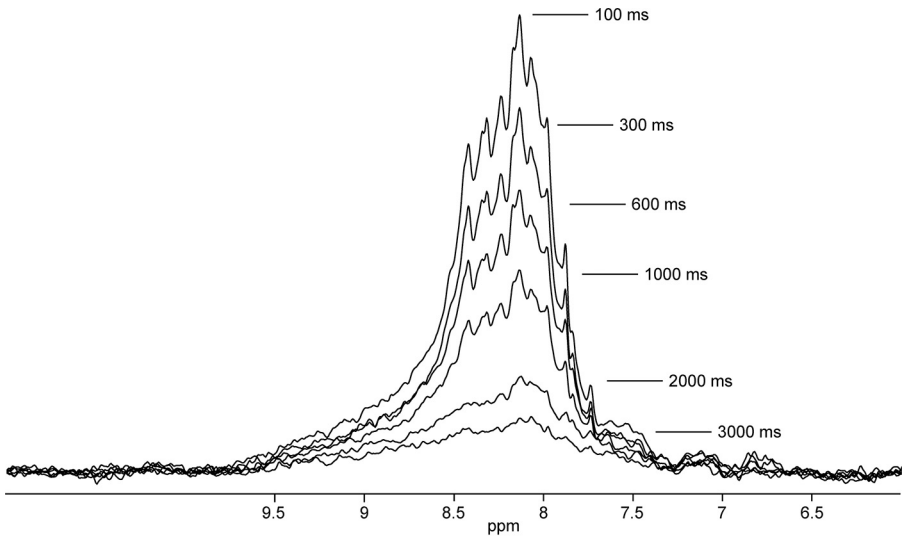

	^{15}N R_1, s^{-1}	^{15}N R_2, s^{-1}	τ_c (app), *ns*	MW (app) *kDa*
WT Hsc70 ADP	0.40 ± 0.03	51 ± 10	29 ± 4	50 ± 8
WT Hsc70 ATP	0.26 ± 0.04	148 ± 25	79 ± 25	130 ± 45
E175S Hsc70 ADP	0.38 ± 0.03	66 ± 10	34 ± 4	62 ± 8
E175S Hsc70 ATP	0.31 ± 0.05	88 ± 5	45 ± 6	85 ± 12

FIGURE 4. **E175S does not undergo interdomain allosteric conformational changes.** ^{1}H-detected ^{15}N-R_1 relaxation for WT Hsc70 (900 MHz) is shown. The relaxation times were 100, 300, 600, 1000, 2000, and 3000 ms (labeled at peak heights). Tabulated results ± uncertainty values (estimated by jackknife procedure (41)) for full-length WT Hsc70 and E175S Hsc70 are shown *below the spectra*.

and a larger apparent molecular weight. For our analysis, we integrated the area $9.5 > {}^1H > 8.7$ ppm only and fitted the decay to single exponential. Error estimation was carried out by a jackknife procedure (41). This approach revealed that there is a large increase in apparent molecular weight for WT Hsc70 in the ATP-bound state (Fig. 4). The conversion used to translate rotational correlation time into molecular weight has been validated for spherical proteins; therefore, the large value seen for the ATP state may be due to the irregular shape of Hsc70. This result suggested that the NBD and SBD are not docked in the ADP-bound state and become docked to each other in the ATP-bound state, as inferred from studies with DnaK, the bacterial Hsc70 ortholog. When we examined E175S Hsc70 using the same methodology, the hydrodynamic properties when bound to ADP were essentially identical to that of WT Hsc70 bound to ADP. However, there was a significantly smaller increase in apparent molecular weight seen in ATP-bound E175S Hsc70 compared with ATP-bound WT Hsc70 (Fig. 4), indicating that the conformation of E175S Hsc70 favors the ADP-bound form regardless of which nucleotide is present. These findings strongly show that the E175S mutation causes Hsc70 to take on DN characteristics; this variant is unable to cycle ATP or refold luciferase despite binding cofactors and substrates appropriately, but it remains permanently in an ADP-bound conformation that has a high affinity for substrate. Thus, the Glu-175 Hsc70 variant appears nearly identical to a chemically inhibited Hsc70 (30), allowing us to test the physiological consequences of Hsc70 selective inhibition in cells.

Mechanism of Selectively Inhibited Hsc70-mediated Tau Clearance—We utilized this new DN-Hsc70 tool to determine how Hsc70 activity affects Tau metabolism and function in a neuronal context. First, we confirmed that in HEK293T cells overexpressing Tau, shRNA-mediated knockdown of Hsc70 clearly reduced Tau levels, as demonstrated previously (28) (Fig. 5*A*). Thus, specific inhibition of Hsc70 promotes Tau clearance. Next, utilizing confocal microscopy of HEK293T cells overexpressing WT or DN-Hsc70-FLAG and RFP-Tau, we found Tau levels were increased in cells expressing WT Hsc70-FLAG and significantly reduced in cells expressing the DN Hsc70-FLAG (Fig. 5*B*). These data confirmed that DN-Hsc70 was not just altering the localization of Tau but was actually facilitating its clearance. Western blot analyses of cells overexpressing WT Hsc70 or DN Hsc70 and Tau confirmed that Tau levels were significantly decreased in the DN-Hsc70-FLAG

FIGURE 3. **Chemical shifts indicate structural rearrangement in E175S Hsc70 nucleotide binding domain.** *A*, overlay of 700 MHz ^{1}H,^{15}N TROSY spectra of Hsc70(1–386) in the ATP state (*red*) and Hsc70(1–386) in the ADP state (*blue*) on 900 MHz ^{1}H,^{15}N TROSY spectra of Hsc70(1–386)E175S in the ATP state (*orange*) and Hsc70(1–386)E175S in the ADP state (*cyan*). The spectra show major differences between the mutant and wild type and no differences between the mutant Hsc70 ATP- and ADP-bound state but significant differences between WT Hsc70 ATP- and ADP-bound state. *B*, enlargement of *A*, The ^{1}H,^{15}N cross-peak for His-227, a residue close to the nucleotide binding site, shifts in the wild type protein between the ATP and ADP state, whereas it does not for Hsc70(1–386)E175S. *C*, 900-MHz ^{1}H,^{15}N TROSY spectra of Hsc70(1–386)E175S in the ATP state (*orange*) and Hsc70(1–386)E175S in the APO state (*green*). *D*, overlay of 900 MHz ^{1}H,^{15}N TROSY spectra of Hsc70(1–386)E175S in the ATP state (*orange*) andHsc70(1–386)E175S in the ADP state (*cyan*). *E*, overlay of 700 MHz ^{1}H,^{15}N TROSY spectra of Hsc70(1–386) in the ATP state (*red*) and Hsc70(1–386) in the ADP state (*blue*). *F*, overlay of 700 MHz ^{1}H,^{15}N TROSY spectra of Hsc70(1–386) in the ADP state (*red*) and Hsc70(1–386) in the APO state (*green*). *G*, NH chemical shift differences between WT-Hsc70 NBD and Glu-175 Hsc70 NBD, both in the ADP-bound state, plotted on the crystal structure of Hsc70 NBD (PDB code 3HSC). Changes in structure mapped on the ribbon structure of Hsc70 NBD reveal E175S induced structural rearrangement in subdomains IA and IIA. *Green*, no change; *yellow*, shift; *red*, loss of resonances; *gray*, no information. *Purple* indicates the location of E175S with ADP and phosphate (*blue*) and a Mg^{2+} ion (*orange*).

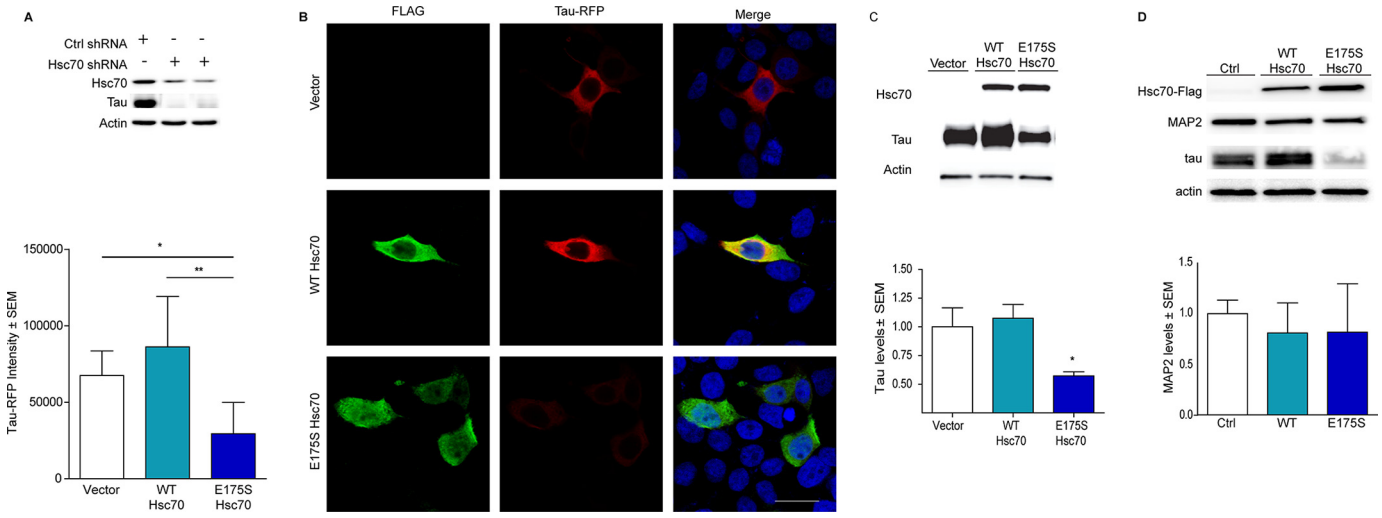

FIGURE 5. **Dominant negative Hsc70 reduces Tau levels.** *A*, Western blot of the effects of shRNA-mediated knockdown of Hsc70 on Tau levels in HEK293T cells. *B*, confocal microscopy of HEK293T cells overexpressing RFP-Tau (*red*) in the presence of vector, WT Hsc70-FLAG, or E175S Hsc70-FLAG (*green*). Confocal z-stack images at 60×; *scale bar* is 10 μm. Quantification of RFP-Tau intensity levels ± S.E. are shown. *, $p < 0.05$, ** $p < 0.01$, one way ANOVA with Tukey's post hoc test for multiple comparisons. C, Western blot of the effects of overexpression of WT and DN Hsc70-FLAG on Tau levels in HEK293T cells. Quantification of Tau levels ± S.E. is shown. *, $p < 0.05$, one way ANOVA. *D*, MAP2 levels in cells overexpressing WT Hsc70 and E175S Hsc70. Quantification of MAP2 levels ± S.E. are shown.

cells (Fig. 5*C*). These effects appeared selective for Tau, as the expression levels of another microtubule-associated protein (MAP), MAP2, were not significantly changed by either WT or DN-Hsc70 overexpression (Fig. 5*D*). We then designed AAV (serotype 9) constructs of WT and DN-Hsc70 to test how Hsc70 activity affected Tau turnover in brain tissue. Hippocampal organotypic slices from FVB-Tg(tetO-MAPT*P301L) mice that produce pathologic mutant human Tau were transduced with GFP AAV9, WT Hsc70-FLAG AAV9, or DN-Hsc70-FLAG AAV9. Confocal microscopy analysis revealed that WT Hsc70 overexpression slightly preserved pathological perikaryal Tau levels above that of GFP in neurons, whereas DN-Hsc70 significantly reduced pathological P301L Tau levels compared with both WT Hsc70 and GFP (Fig. 6).

Because pan-Hsp70 inhibitors triage Tau to Hsp90 for proteasomal degradation (30, 51), we speculated that DN-Hsc70 was similarly triaging Tau. Indeed, Tau immunoprecipitated from cells overexpressing DN-Hsc70 is associated with more Hsp90 compared with WT Hsc70 (Fig. 7*A*). We then confirmed that DN-Hsc70 is triaging Tau by the proteasome by treating cells overexpressing WT or DN-Hsc70 with the proteasome inhibitor epoxomicin for 6 h. Tau degradation caused by DN-Hsc70 was completely blocked by epoxomicin (Fig. 7*B*). Conversely, Tau degradation by DN-Hsc70 did not occur through autophagy, as siRNA targeting the autophagy mediator, Beclin-1 (Fig. 7*C*), did not block Tau reductions by DN-Hsc70. Thus, in the neuronal and cellular context, isoform-selective inhibition of Hsc70 causes similar effects to that of small molecule pan-Hsp70 inhibitors with regard to Tau biology (30).

DN-Hsc70 Has an Altered Co-chaperone Complement—We then sought to determine a putative cellular mechanism for this dramatic shift in Hsc70 function caused by the E175S mutation. Given that DN-Hsc70 efficiently degraded Tau in cells compared with WT Hsc70, we speculated that the chaperone interactome (chaperome) bound to DN-Hsc70 was distinct from WT Hsc70. WT or DN-Hsc70 were co-immunoprecipitated

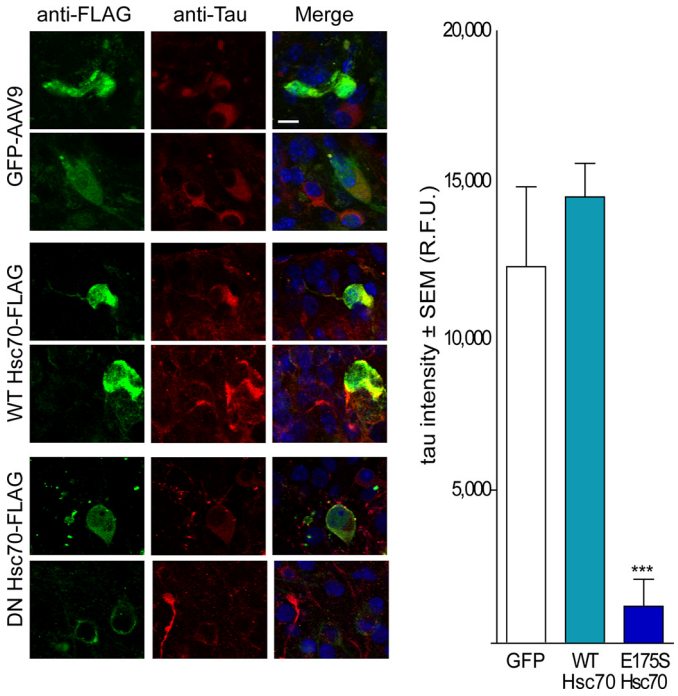

FIGURE 6. **DN Hsc70 facilitates Tau degradation in neurons.** Tau levels in organotypic hippocampal slices from FVB-Tg(tetO-MAPT*P301L) mice transduced with either AAV9-GFP, WT Hsc70-FLAG, or E175S Hsc70-FLAG and immunostained with anti-FLAG (*green*), anti-Tau H150 (*red*), and DAPI (*blue*). The *scale bar* is 10 μm (60× objective with 2× zoom). Data are the mean intensity ± S.E.; $n = 10$; ***, $p < 0.001$, one-way ANOVA.

from HEK cell lysates and analyzed by HPLC-MS/MS to identify the most robust interactors of each variant. As predicted, these interacting partners were predominantly co-chaperones and other chaperones. Co-chaperones such as CHIP, HIP, and HOP bound either variant similarly. Interestingly, WT Hsc70 tended toward increased interaction with other Hsp70 isoforms, whereas DN-Hsc70 had increased association with several DnaJ proteins and Hsp90 isoforms (Fig. 8*A*). We confirmed

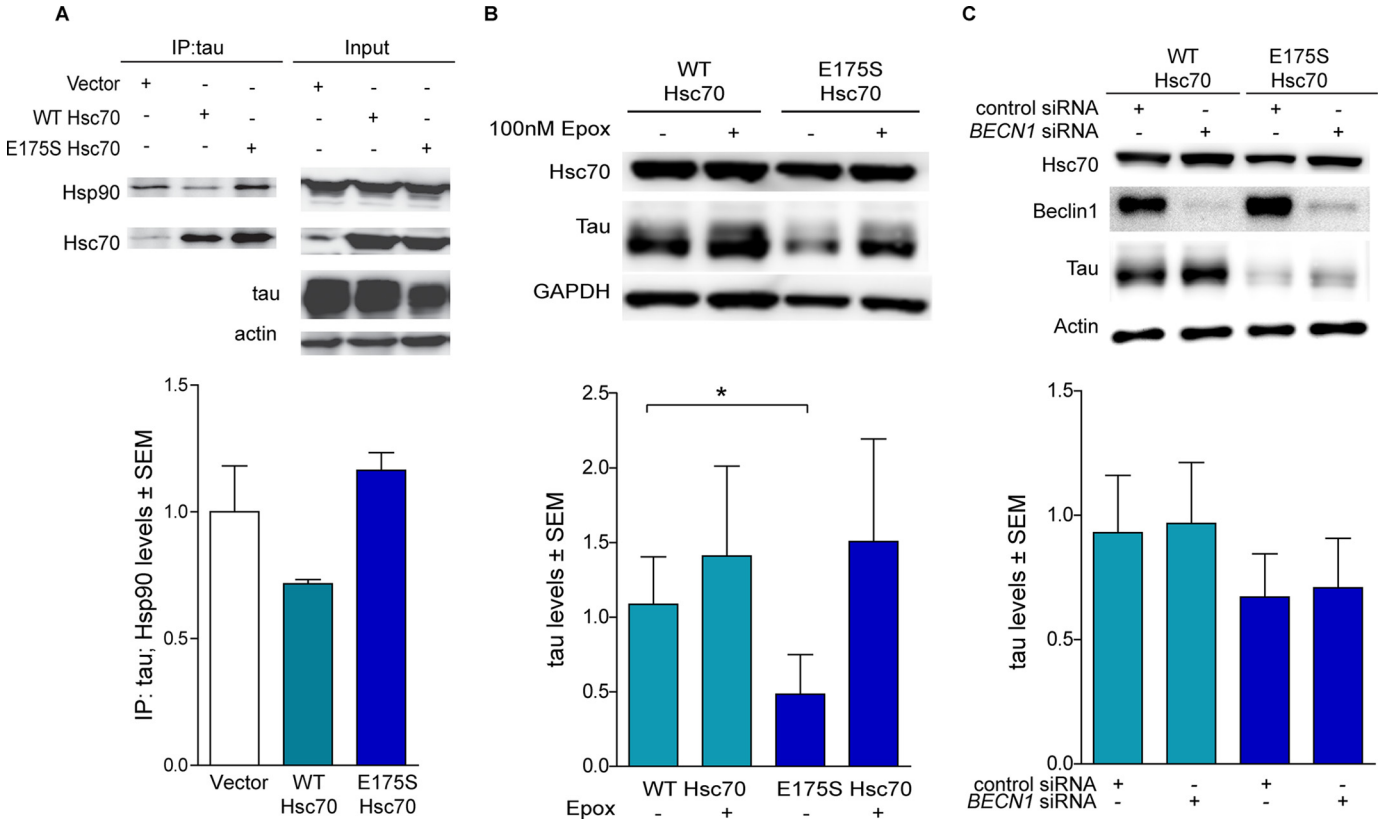

FIGURE 7. **DN Hsc70 degrades Tau via the proteasome.** *A*, Western blot image of Tau immunoprecipitated (*IP*) from cells expressing vector, WT Hsc70, or E175S. Shown is quantification of Hsp90 levels in the Tau immunoprecipitation; data are the mean ± S.E. *B*, Western blot of Tau levels in HEK293T cells transfected with WT Tau and a transfection control, Hsc70 WT, or Hsc70 E175S after inhibition of the proteasome by 6 h of epoxomicin treatment. Quantification data are the mean ± S.E., $n = 4$, *, $p < 0.05$. *C*, Western blot of inhibition of macroautophagy by Beclin1 knockdown; at least 60% knockdown was achieved with the siRNA. Quantification is the mean ± S.E., $n = 3$.

these interactions by immunoprecipitating WT or E175S Hsc70 and probing for levels of bound DnaJA1 and DnaJC7 (Fig. 8*B*). Thus, the DN-Hsc70 variant, which is locked into an ADP-bound conformation, prevents the dissociation of DnaJs and abrogates the interaction with other Hsp70 family members, promoting the recruitment of Hsp90 to the complex to facilitate Tau degradation.

Discussion

Here we sought to determine the impact of selective Hsc70 inhibition on the stability of the microtubule associated protein Tau. Chaperone modulation holds great promise as a potential therapeutic for tauopathies and can allow us to better understand the biology of Tau as it relates to both its normal and pathogenic functions. Hsc70 in particular seems to be a key regulator of Tau biology in the brain, warranting the pursuit of strategies aimed at disrupting this chaperone/client interface. In this study, using genetic and biochemical approaches, we determined that isoform-selective inhibition of the most abundant Hsp70 family member, Hsc70, can dramatically enhance Tau clearance, similar to what has previously been observed with small molecule pan Hsp70 inhibitors. Almost identically to these inhibitors, the E175S Hsc70 variant took on DN properties when overexpressed in cells that led to Tau degradation through the proteasome by recruiting Hsp90 proteins (52).

The E175S Hsc70 had nearly normal affinity for nucleotides and co-chaperones yet lacked essential ATPase and luciferase refolding activities, features that were previously unknown for this variant with regard to human Hsc70 (43, 44, 53, 54). Human Hsc70 is also thought to undergo major conformational changes within its subdomains in response to co-chaperone binding and nucleotide hydrolysis in a manner similar to Hsp70 proteins from other species (48, 55–60), but this also remained unknown until the NMR analyses in these studies. Differences in several resonances in subdomains IA and IIA caused by the E175S Hsc70 confirm that this mutation alters the allosteric communication between the SBD and NBD of Hsc70, dramatically impacting its function. This is consistent with previous work showing that the cleft between these subdomains is important for relaying initial NBD conformational changes to the SBD in bacterial Hsp70, DnaK (48, 58, 60, 61). Interestingly, NMR of full-length E175S Hsc70 also showed that the ADP-bound conformation was essentially identical to that of WT Hsc70; however, E175S Hsc70 was unresponsive to the conformational changes typically caused by ATP/ADP exchange as demonstrated by ^{15}N relaxation time measurements. Thus, the E175S mutation in Hsc70 locked this chaperone into an ADP-bound state regardless of which nucleotide was bound within the NBD, again almost perfectly mimicking Hsc70 in the presence of a small molecule pan Hsp70 allosteric modulator.

This tool also allowed us to shed new light on how ATPase chaperone scaffolds like Hsc70 make triage decisions (62–65). Our LC-MS/MS results indicate that chaperone/chaperone

A

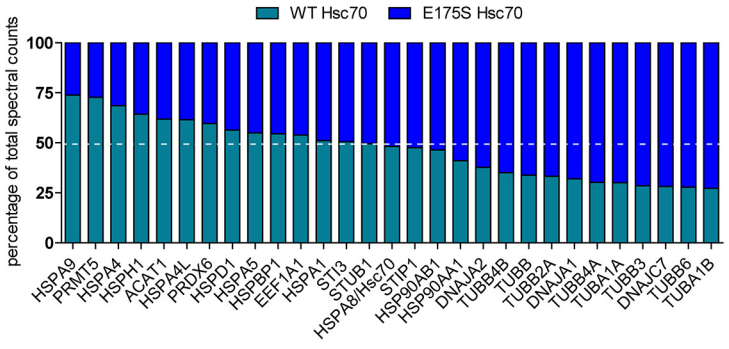

	Protein	Average Spectral Count E175S Hsc70	Average Spectral Count WT Hsc70	Fold Change (Mutant/WT)	G-test (p-value)
Enriched in E175S	TUBA1B	133.00	49.67	2.68	3.35×10^{-10}
	TUBB6	17.33	6.67	2.60	0.0268
	DNAJC7	23.00	9.00	2.56	0.0118
	TUBB3	45.00	18.00	2.50	0.0005
	TUBA1A	145.00	62.33	2.33	5.18×10^{-9}
	TUBB4A	57.67	25.00	2.31	0.0003
	DNAJA1	22.00	10.33	2.13	0.0379
	TUBB2A	56.00	28.00	2.00	0.0020
	TUBB	84.33	43.00	1.96	0.0002
	TUBB4B	68.33	37.00	1.85	0.3005
	DNAJA2	11.00	6.67	1.65	0.0803
	HSP90AA1	56.00	39.00	1.44	0.4348
	HSP90AB1	66.00	57.33	1.15	0.9559
No change	HSPA8/Hsc70	1251.33	1166.67	1.07	0.0851
	STI3	14.67	14.33	1.02	0.9497
	STUB1	17.67	18.00	0.98	0.9559
	HSPA1	255.33	267.00	0.96	0.6096
	STIP1	16.33	18.00	0.91	0.7756
Enriched in WT	EEF1A1	38.00	44.33	0.86	0.4852
	HSPBP1	36.67	44.00	0.83	0.4141
	HSPA5	57.67	70.33	0.82	0.2628
	HSPD1	16.00	20.67	0.77	0.4340
	PRDX6	7.67	11.33	0.68	0.3996
	HSPA4L	23.33	37.33	0.63	0.0710
	ACAT1	7.00	11.33	0.62	0.3096
	HSPH1	22.00	39.67	0.55	0.0235
	HSPA4	73.00	159.33	0.46	9.90×10^{-9}
	PRMT5	6.00	16.00	0.38	0.0299
	HSPA9	7.67	21.67	0.35	0.0083

B

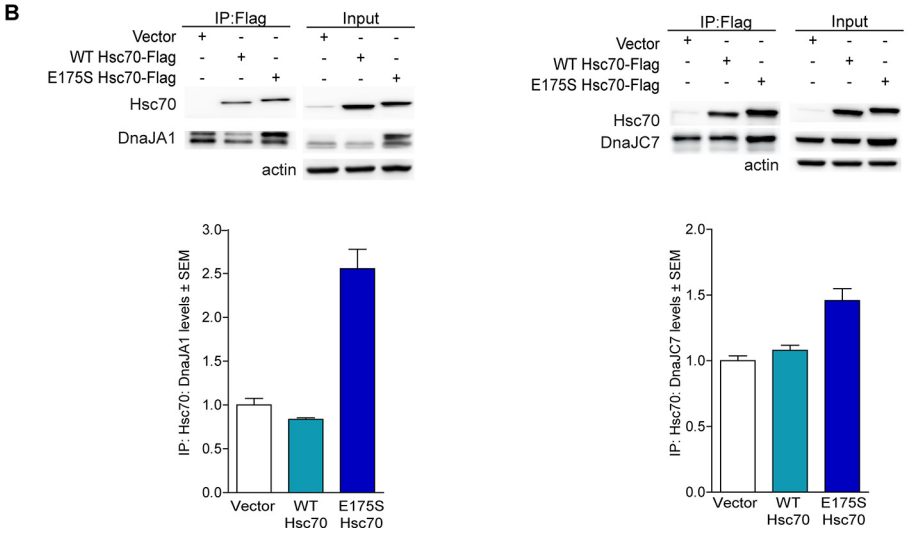

FIGURE 8. **Mass spec reveals a changing chaperome for DN Hsc70 compared with WT Hsc70.** *A*, average spectral counts plotted as percentages to illustrate whether a protein was enriched in WT (*cyan*) or E175S Hsc70 (*blue*). Data are the averages of three independent mass spectroscopy experiments. Results that were <10 spectral counts in either sample were discarded to ensure robustness of the results. *B*, confirmation of mass spectroscopy results; representative Western blot images of Tau immunoprecipitated (*IP*) from cells overexpressing Hsc70 WT Hsc70 or E175S Hsc70 and probed for DnaJA1 and DnaJC7 is shown.

and chaperone/co-chaperone dynamics change based on nucleotide exchange, providing deeper insight into how client fate is decided. Hsc70 that is locked into an ADP-bound conformation prevents DnaJ proteins from cycling off, recruiting Hsp90 proteins to promote client clearance. Our MS results also unexpectedly suggested an important role for Hsc70 nucleotide exchange in microtubule dynamics as a number of tubulin proteins had higher association with DN-Hsc70 relative to WT. This not only provides even greater evidence for a functional link between the microtubule-associated protein Tau and Hsc70, as previously suggested (20), but it also suggests that a major role of Hsc70 could be regulation of microtubule dynamics. Hsc70 has been associated with functions that require microtubules, such as spindle formation (66) and regulation of axonal transport along microtubules (67, 68). Our results here show that these functions are likely critically linked to Hsc70 activity. Another interesting and unexpected result from these MS studies was the finding that WT Hsc70 interacted with other Hsp70 isoforms in the cell, but in the absence of allosteric changes caused by nucleotide exchange these interactions were prevented, as demonstrated by the results with E175S Hsc70. Perhaps nucleotide-induced conformational changes in Hsp70 proteins are essential for intracompartmental trafficking of properly folded proteins in cells. Regardless, these results suggest that intradomain allosteric changes are essential for Hsc70 to interact with other Hsp70 isoforms to coordinate proteostasis, an area that has yet to be explored in depth in the chaperone field.

With regard to Tau pathobiology, our results here prove what we previously could only speculate: that Hsc70 is an excel-

lent therapeutic target for tauopathies with regard to efficacy and perhaps even specificity. We previously showed that Hsc70 preserved Tau levels in cells and that the aged human brain had high levels of Hsc70 (20, 28), but it remained unknown if Hsc70 could be targeted to promote Tau clearance in neurons and whether such a strategy was practical given the important role of Hsc70 in a number of cellular processes. By identifying and using the E175S Hsc70 variant, we were able to address both of these issues to some extent. First, overexpression of the E175S Hsc70 variant was not fatal to cells or neurons, suggesting that some perturbation of Hsc70 may be permissible, at least acutely. Second, we prove for the first time in neurons that targeting the activity of a single Hsp70 isoform, Hsc70, is a very potent anti-Tau strategy. Inhibitors that generically target all isoforms of Hsp70, while effective at lowering Tau (29, 30), will undoubtedly have more untoward consequences in neurons compared with isoform-selective inhibitors. This is because several Hsp70 isoforms are critical for basic cellular function. For example, targeting BiP/Grp78 would disrupt endoplasmic reticulum protein quality control and induce the unfolded protein response (69, 70). Targeting mortalin would certainly impact mitochondrial function and lead to neuronal death (71). And although targeting Hsc70 may also be deleterious given its important role in cellular homeostasis, our results suggest that there is some level of flexibility built into the proteostasis system that could allow for a chemotherapeutic approach targeting this Hsp70 isoform to treat tauopathies and possibly other neurodegenerative diseases. Therefore, the design and development of Hsp70 isoform-selective inhibitors will likely be essential for rationally targeting these proteins for therapeutic purposes in the future, and although challenging due to structural similarities between Hsp70 isoforms, it is possible. An Hsp72-selective inhibitor was recently developed and showed good efficacy for treating cancer with fewer side effects (72). Development of Hsc70 selective inhibitors could hold similar promise for tauopathies.

In conclusion, using a DN-Hsc70, we have proven that targeting this Hsp70 isoform contributes to the majority of anti-Tau activity seen with small molecule pan Hsp70 inhibitors. This DN-Hsc70 causes Tau degradation through the same Hsp90/proteasome mechanism as that engaged by such Hsp70 inhibitors (30). DN-Hsc70 lacks the conformational dynamics induced by nucleotide exchange in Hsc70 protein, locking Hsc70 into a high affinity state for substrates that promotes client degradation. Client degradation appears critically linked to fluidity in the DnaJ-Hsc70 complex, such that if DnaJ proteins are unable to decouple from Hsc70, Hsp90 is recruited to this complex to promote client turnover. Our data show that selective inhibition of Hsc70 activity could be tractable for treating tauopathies and elucidating the mechanisms of Tau metabolism as well as the metabolism of other clients of this important chaperone protein.

Acknowledgments—This is the result of work supported with resources and the use of facilities at the James A. Haley Veterans' Hospital. We thank Dr. Byeong Cha for assistance with microscopy.

References

1. Palleros, D. R., Reid, K. L., Shi, L., Welch, W. J., and Fink, A. L. (1993) ATP-induced protein-Hsp70 complex dissociation requires K^+ but not ATP hydrolysis. *Nature* **365,** 664–666
2. Cheetham, M. E., Jackson, A. P., and Anderton, B. H. (1994) Regulation of 70-kDa heat-shock-protein ATPase activity and substrate binding by human DnaJ-like proteins, HSJ1a and HSJ1b. *Eur. J. Biochem.* **226,** 99–107
3. Wittung-Stafshede, P., Guidry, J., Horne, B. E., and Landry, S. J. (2003) The J-domain of Hsp40 couples ATP hydrolysis to substrate capture in Hsp70. *Biochemistry* **42,** 4937–4944
4. McKay, D. B. (1993) Structure and mechanism of 70-kDa heat-shock-related proteins. *Adv. Protein Chem.* **44,** 67–98
5. Mayer, M. P. (2010) Gymnastics of molecular chaperones. *Mol. Cell* **39,** 321–331
6. Tavaria, M., Gabriele, T., Kola, I., and Anderson, R. L. (1996) A hitchhiker's guide to the human Hsp70 family. *Cell Stress Chaperones* **1,** 23–28
7. Brocchieri, L., Conway de Macario, E., and Macario, A. J. (2008) hsp70 genes in the human genome: conservation and differentiation patterns predict a wide array of overlapping and specialized functions. *BMC Evol. Biol.* **8,** 19
8. Zylicz, M., and Wawrzynow, A. (2001) Insights into the function of Hsp70 chaperones. *IUBMB life* **51,** 283–287
9. Schmid, S. L., Braell, W. A., and Rothman, J. E. (1985) ATP catalyzes the sequestration of clathrin during enzymatic uncoating. *J. Biol. Chem.* **260,** 10057–10062
10. Chappell, T. G., Welch, W. J., Schlossman, D. M., Palter, K. B., Schlesinger, M. J., and Rothman, J. E. (1986) Uncoating ATPase is a member of the 70-kilodalton family of stress proteins. *Cell* **45,** 3–13
11. Dworniczak, B., and Mirault, M. E. (1987) Structure and expression of a human gene coding for a 71-kDa heat shock "cognate" protein. *Nucleic Acids Res.* **15,** 5181–5197
12. Chamberlain, L. H., and Burgoyne, R. D. (1997) Activation of the ATPase activity of heat-shock proteins Hsc70/Hsp70 by cysteine-string protein. *Biochem. J.* **322,** 853–858
13. Rajapandi, T., Greene, L. E., and Eisenberg, E. (2000) The molecular chaperones Hsp90 and Hsc70 are both necessary and sufficient to activate hormone binding by glucocorticoid receptor. *J. Biol. Chem.* **275,** 22597–22604
14. Joglekar, A. P., and Hay, J. C. (2005) Evidence for regulation of ER/Golgi SNARE complex formation by hsc70 chaperones. *Eur. J. Cell Biol.* **84,** 529–542
15. Panjwani, N., Akbari, O., Garcia, S., Brazil, M., and Stockinger, B. (1999) The HSC73 molecular chaperone: involvement in MHC class II antigen presentation. *J. Immunol.* **163,** 1936–1942
16. Turturici, G., Geraci, F., Candela, M. E., Giudice, G., Gonzalez, F., and Sconzo, G. (2008) Hsp70 localizes differently from chaperone Hsc70 in mouse mesoangioblasts under physiological growth conditions. *J. Mol. Histol.* **39,** 571–578
17. Yuan, A., Mills, R. G., Chia, C. P., and Bray, J. J. (2000) Tubulin and neurofilament proteins are transported differently in axons of chicken motoneurons. *Cell. Mol. Neurobiol.* **20,** 623–632
18. Dou, F., Netzer, W. J., Tanemura, K., Li, F., Hartl, F. U., Takashima, A., Gouras, G. K., Greengard, P., and Xu, H. (2003) Chaperones increase association of Tau protein with microtubules. *Proc. Natl. Acad. Sci. U.S.A.* **100,** 721–726
19. Sarkar, M., Kuret, J., and Lee, G. (2008) Two motifs within the Tau microtubule-binding domain mediate its association with the hsc70 molecular chaperone. *J. Neurosci. Res.* **86,** 2763–2773
20. Jinwal, U. K., O'Leary, J. C., 3rd, Borysov, S. I., Jones, J. R., Li, Q., Koren, J., 3rd, Abisambra, J. F., Vestal, G. D., Lawson, L. Y., Johnson, A. G., Blair, L. J., Jin, Y., Miyata, Y., Gestwicki, J. E., and Dickey, C. A. (2010) Hsc70 rapidly engages Tau after microtubule destabilization. *J. Biol. Chem.* **285,** 16798–16805
21. Panda, D., Samuel, J. C., Massie, M., Feinstein, S. C., and Wilson, L. (2003) Differential regulation of microtubule dynamics by three- and four-repeat Tau: implications for the onset of neurodegenerative disease. *Proc. Natl. Acad. Sci. U.S.A.* **100,** 9548–9553

22. Bunker, J. M., Wilson, L., Jordan, M. A., and Feinstein, S. C. (2004) Modulation of microtubule dynamics by Tau in living cells: implications for development and neurodegeneration. *Mol. Biol. Cell* **15,** 2720–2728
23. Choi, M. C., Raviv, U., Miller, H. P., Gaylord, M. R., Kiris, E., Ventimiglia, D., Needleman, D. J., Kim, M. W., Wilson, L., Feinstein, S. C., and Safinya, C. R. (2009) Human microtubule-associated-protein Tau regulates the number of protofilaments in microtubules: a synchrotron x-ray scattering study. *Biophys. J.* **97,** 519–527
24. Kosik, K. S., Joachim, C. L., and Selkoe, D. J. (1986) Microtubule-associated protein Tau (Tau) is a major antigenic component of paired helical filaments in Alzheimer disease. *Proc. Natl. Acad. Sci. U.S.A.* **83,** 4044–4048
25. Rosso, S. M., van Herpen, E., Deelen, W., Kamphorst, W., Severijnen, L. A., Willemsen, R., Ravid, R., Niermeijer, M. F., Dooijes, D., Smith, M. J., Goedert, M., Heutink, P., and van Swieten, J. C. (2002) A novel Tau mutation, S320F, causes a tauopathy with inclusions similar to those in Pick's disease. *Ann. Neurol.* **51,** 373–376
26. Arriagada, P. V., Growdon, J. H., Hedley-Whyte, E. T., and Hyman, B. T. (1992) Neurofibrillary tangles but not senile plaques parallel duration and severity of Alzheimer's disease. *Neurology* **42,** 631–639
27. Santacruz, K., Lewis, J., Spires, T., Paulson, J., Kotilinek, L., Ingelsson, M., Guimaraes, A., DeTure, M., Ramsden, M., McGowan, E., Forster, C., Yue, M., Orne, J., Janus, C., Mariash, A., Kuskowski, M., Hyman, B., Hutton, M., and Ashe, K. H. (2005) Tau suppression in a neurodegenerative mouse model improves memory function. *Science* **309,** 476–481
28. Jinwal, U. K., Akoury, E., Abisambra, J. F., O'Leary, J. C., 3rd, Thompson, A. D., Blair, L. J., Jin, Y., Bacon, J., Nordhues, B. A., Cockman, M., Zhang, J., Li, P., Zhang, B., Borysov, S., Uversky, V. N., Biernat, J., Mandelkow, E., Gestwicki, J. E., Zweckstetter, M., and Dickey, C. A. (2013) Imbalance of Hsp70 family variants fosters Tau accumulation. *FASEB J.* **27,** 1450–1459
29. Miyata, Y., Li, X., Lee, H. F., Jinwal, U. K., Srinivasan, S. R., Seguin, S. P., Young, Z. T., Brodsky, J. L., Dickey, C. A., Sun, D., and Gestwicki, J. E. (2013) Synthesis and initial evaluation of YM-08, a blood-brain barrier permeable derivative of the heat shock protein 70 (Hsp70) inhibitor MKT-077, which reduces Tau levels. *ACS Chem. Neurosci.* **4,** 930–939
30. Abisambra, J., Jinwal, U. K., Miyata, Y., Rogers, J., Blair, L., Li, X., Seguin, S. P., Wang, L., Jin, Y., Bacon, J., Brady, S., Cockman, M., Guidi, C., Zhang, J., Koren, J., Young, Z. T., Atkins, C. A., Zhang, B., Lawson, L. Y., Weeber, E. J., Brodsky, J. L., Gestwicki, J. E., and Dickey, C. A. (2013) Allosteric heat shock protein 70 inhibitors rapidly rescue synaptic plasticity deficits by reducing aberrant Tau. *Biol. Psychiatry* **74,** 367–374
31. Kang, Y., Taldone, T., Patel, H. J., Patel, P. D., Rodina, A., Gozman, A., Maharaj, R., Clement, C. C., Patel, M. R., Brodsky, J. L., Young, J. C., and Chiosis, G. (2014) Heat shock protein 70 inhibitors. 1. 2,5′-thiodipyrimidine and 5-(phenylthio)pyrimidine acrylamides as irreversible binders to an allosteric site on heat shock protein 70. *J. Med. Chem.* **57,** 1188–1207
32. Rodina, A., Patel, P. D., Kang, Y., Patel, Y., Baaklini, I., Wong, M. J., Taldone, T., Yan, P., Yang, C., Maharaj, R., Gozman, A., Patel, M. R., Patel, H. J., Chirico, W., Erdjument-Bromage, H., Talele, T. T., Young, J. C., and Chiosis, G. (2013) Identification of an allosteric pocket on human hsp70 reveals a mode of inhibition of this therapeutically important protein. *Chem. Biol.* **20,** 1469–1480
33. Rousaki, A., Miyata, Y., Jinwal, U. K., Dickey, C. A., Gestwicki, J. E., and Zuiderweg, E. R. (2011) Allosteric drugs: the interaction of antitumor compound MKT-077 with human Hsp70 chaperones. *J. Mol. Biol.* **411,** 614–632
34. Taldone, T., Kang, Y., Patel, H. J., Patel, M. R., Patel, P. D., Rodina, A., Patel, Y., Gozman, A., Maharaj, R., Clement, C. C., Lu, A., Young, J. C., and Chiosis, G. (2014) Heat shock protein 70 inhibitors. 2. 2,5′-thiodipyrimidines, 5-(phenylthio)pyrimidines, 2-(pyridin-3-ylthio)pyrimidines, and 3-(phenylthio)pyridines as reversible binders to an allosteric site on heat shock protein 70. *J. Med. Chem.* **57,** 1208–1224
35. Wisén, S., Androsavich, J., Evans, C. G., Chang, L., and Gestwicki, J. E. (2008) Chemical modulators of heat shock protein 70 (Hsp70) by sequential, microwave-accelerated reactions on solid phase. *Bioorg. Med. Chem. Lett.* **18,** 60–65
36. Schlecht, R., Scholz, S. R., Dahmen, H., Wegener, A., Sirrenberg, C., Musil, D., Bomke, J., Eggenweiler, H. M., Mayer, M. P., and Bukau, B. (2013) Functional analysis of Hsp70 inhibitors. *PloS ONE* **8,** e78443
37. Rauch, J. N., and Gestwicki, J. E. (2014) Binding of human nucleotide exchange factors to heat shock protein 70 (Hsp70) generates functionally distinct complexes in vitro. *J. Biol. Chem.* **289,** 1402–1414
38. Chang, L., Bertelsen, E. B., Wisén, S., Larsen, E. M., Zuiderweg, E. R., and Gestwicki, J. E. (2008) High-throughput screen for small molecules that modulate the ATPase activity of the molecular chaperone DnaK. *Anal. Biochem.* **372,** 167–176
39. Miyata, Y., Chang, L., Bainor, A., McQuade, T. J., Walczak, C. P., Zhang, Y., Larsen, M. J., Kirchhoff, P., and Gestwicki, J. E. (2010) High-throughput screen for *Escherichia coli* heat shock protein 70 (Hsp70/DnaK): ATPase assay in low volume by exploiting energy transfer. *J. Biomol. Screen.* **15,** 1211–1219
40. Wisén, S., and Gestwicki, J. E. (2008) Identification of small molecules that modify the protein folding activity of heat shock protein 70. *Anal. Biochem.* **374,** 371–377
41. Quenouille, M. H. (1956) Notes on bias in estimation. *Biometrika* **43,** 353–360, 10.1093/biomet/43.3–4.353
42. Gogolla, N., Galimberti, I., DePaola, V., and Caroni, P. (2006) Staining protocol for organotypic hippocampal slice cultures. *Nat. Protoc.* **1,** 2452–2456
43. Flaherty, K. M., Wilbanks, S. M., DeLuca-Flaherty, C., and McKay, D. B. (1994) Structural basis of the 70-kilodalton heat shock cognate protein ATP hydrolytic activity. II. Structure of the active site with ADP or ATP bound to wild type and mutant ATPase fragment. *J. Biol. Chem.* **269,** 12899–12907
44. Wilbanks, S. M., DeLuca-Flaherty, C., and McKay, D. B. (1994) Structural basis of the 70-kilodalton heat shock cognate protein ATP hydrolytic activity. I. Kinetic analyses of active site mutants. *J. Biol. Chem.* **269,** 12893–12898
45. Johnson, E. R., and McKay, D. B. (1999) Mapping the role of active site residues for transducing an ATP-induced conformational change in the bovine 70-kDa heat shock cognate protein. *Biochemistry* **38,** 10823–10830
46. Ricci, L., and Williams, K. P. (2008) Development of fluorescence polarization assays for the molecular chaperone Hsp70 family members: Hsp72 and DnaK. *Curr. Chem. genomics* **2,** 90–95
47. Swain, J. F., Dinler, G., Sivendran, R., Montgomery, D. L., Stotz, M., and Gierasch, L. M. (2007) Hsp70 chaperone ligands control domain association via an allosteric mechanism mediated by the interdomain linker. *Mol. Cell* **26,** 27–39
48. Zhuravleva, A., and Gierasch, L. M. (2011) Allosteric signal transmission in the nucleotide-binding domain of 70-kDa heat shock protein (Hsp70) molecular chaperones. *Proc. Natl. Acad. Sci. U.S.A.* **108,** 6987–6992
49. Cavanagh, J., Fairbrother, W., Palmer AGIII, R. M., and Skeleton, N. (2007) *Protein NMR Spectroscopy: Principles and Practice*, 2nd Ed., pp. 679–724, Academic Press, Amsterdam
50. Cavanagh, J., Fairbrother, W., Palmer, A. G., 3rd, Rance, M., and Skelton, N. J. (2007) *Protein NMR Spectroscopy: Principles and Practice*, 2nd ed., pp. 725–780, Elsevier Academic Press, Amsterdam
51. Wang, Y., and Mandelkow, E. (2012) Degradation of Tau protein by autophagy and proteasomal pathways. *Biochem. Soc. Trans.* **40,** 644–652
52. Thompson, A. D., Scaglione, K. M., Prensner, J., Gillies, A. T., Chinnaiyan, A., Paulson, H. L., Jinwal, U. K., Dickey, C. A., and Gestwicki, J. E. (2012) Analysis of the Tau-associated proteome reveals that exchange of Hsp70 for Hsp90 is involved in Tau degradation. *ACS Chem. Biol.* **7,** 1677–1686
53. O'Brien, M. C., Flaherty, K. M., and McKay, D. B. (1996) Lysine 71 of the chaperone protein Hsc70 is essential for ATP hydrolysis. *J. Biol. Chem.* **271,** 15874–15878
54. O'Brien, M. C., and McKay, D. B. (1993) Threonine 204 of the chaperone protein Hsc70 influences the structure of the active site, but is not essential for ATP hydrolysis. *J. Biol. Chem.* **268,** 24323–24329
55. Liberek, K., Skowyra, D., Zylicz, M., Johnson, C., and Georgopoulos, C. (1991) The *Escherichia coli* DnaK chaperone, the 70-kDa heat shock protein eukaryotic equivalent, changes conformation upon ATP hydrolysis, thus triggering its dissociation from a bound target protein. *J. Biol. Chem.* **266,** 14491–14496
56. Zhuravleva, A., Clerico, E. M., and Gierasch, L. M. (2012) An interdomain energetic tug-of-war creates the allosterically active state in Hsp70 molec-

ular chaperones. *Cell* **151,** 1296–1307
57. General, I. J., Liu, Y., Blackburn, M. E., Mao, W., Gierasch, L. M., and Bahar, I. (2014) ATPase subdomain IA is a mediator of interdomain allostery in Hsp70 molecular chaperones. *PLoS Comput. Biol.* **10,** e1003624
58. Zhang, Y., and Zuiderweg, E. R. (2004) The 70-kDa heat shock protein chaperone nucleotide-binding domain in solution unveiled as a molecular machine that can reorient its functional subdomains. *Proc. Natl. Acad. Sci. U.S.A.* **101,** 10272–10277
59. Bhattacharya, A., Kurochkin, A. V., Yip, G. N., Zhang, Y., Bertelsen, E. B., and Zuiderweg, E. R. (2009) Allostery in Hsp70 chaperones is transduced by subdomain rotations. *J. Mol. Biol.* **388,** 475–490
60. Bertelsen, E. B., Chang, L., Gestwicki, J. E., and Zuiderweg, E. R. (2009) Solution conformation of wild-type *E. coli* Hsp70 (DnaK) chaperone complexed with ADP and substrate. *Proc. Natl. Acad. Sci. U.S.A.* **106,** 8471–8476
61. Kityk, R., Kopp, J., Sinning, I., and Mayer, M. P. (2012) Structure and dynamics of the ATP-bound open conformation of Hsp70 chaperones. *Mol. Cell* **48,** 863–874
62. Stankiewicz, M., Nikolay, R., Rybin, V., and Mayer, M. P. (2010) CHIP participates in protein triage decisions by preferentially ubiquitinating Hsp70-bound substrates. *FEBS J.* **277,** 3353–3367
63. Connell, P., Ballinger, C. A., Jiang, J., Wu, Y., Thompson, L. J., Höhfeld, J., and Patterson, C. (2001) The co-chaperone CHIP regulates protein triage decisions mediated by heat-shock proteins. *Nat. Cell Biol.* **3,** 93–96
64. Shiber, A., Breuer, W., Brandeis, M., and Ravid, T. (2013) Ubiquitin conjugation triggers misfolded protein sequestration into quality control foci when Hsp70 chaperone levels are limiting. *Mol. Biol. Cell* **24,** 2076–2087
65. Marques, C., Guo, W., Pereira, P., Taylor, A., Patterson, C., Evans, P. C., and Shang, F. (2006) The triage of damaged proteins: degradation by the ubiquitin-proteasome pathway or repair by molecular chaperones. *FASEB J.* **20,** 741–743
66. Agueli, C., Geraci, F., Giudice, G., Chimenti, L., Cascino, D., and Sconzo, G. (2001) A constitutive 70 kDa heat-shock protein is localized on the fibres of spindles and asters at metaphase in an ATP-dependent manner: a new chaperone role is proposed. *Biochem. J.* **360,** 413–419
67. Terada, S., Kinjo, M., Aihara, M., Takei, Y., and Hirokawa, N. (2010) Kinesin-1/Hsc70-dependent mechanism of slow axonal transport and its relation to fast axonal transport. *EMBO J.* **29,** 843–854
68. Tsai, M. Y., Morfini, G., Szebenyi, G., and Brady, S. T. (2000) Release of kinesin from vesicles by hsc70 and regulation of fast axonal transport. *Mol. Biol. Cell* **11,** 2161–2173
69. Zhang, Y., Liu, R., Ni, M., Gill, P., and Lee, A. S. (2010) Cell surface relocalization of the endoplasmic reticulum chaperone and unfolded protein response regulator GRP78/BiP. *J. Biol. Chem.* **285,** 15065–15075
70. Li, J., Ni, M., Lee, B., Barron, E., Hinton, D. R., and Lee, A. S. (2008) The unfolded protein response regulator GRP78/BiP is required for endoplasmic reticulum integrity and stress-induced autophagy in mammalian cells. *Cell Death Differ.* **15,** 1460–1471
71. Liu, Y., Liu, W., Song, X. D., and Zuo, J. (2005) Effect of GRP75/mthsp70/PBP74/mortalin overexpression on intracellular ATP level, mitochondrial membrane potential, and ROS accumulation following glucose deprivation in PC12 cells. *Mol. Cell. Biochem.* **268,** 45–51
72. Howe, M. K., Bodoor, K., Carlson, D. A., Hughes, P. F., Alwarawrah, Y., Loiselle, D. R., Jaeger, A. M., Darr, D. B., Jordan, J. L., Hunter, L. M., Molzberger, E. T., Gobillot, T. A., Thiele, D. J., Brodsky, J. L., Spector, N. L., and Haystead, T. A. (2014) Identification of an allosteric small-molecule inhibitor selective for the inducible form of heat shock protein 70. *Chem. Biol.* **21,** 1648–1659